Thermal Testing and Analysis of an Efficient High-Temperature Multi-screen Internal Insulation

Stefan Weiland

Karin Handrick

Kamran Daryabeigi

ABSTRACT

Conventional multi-layer insulations exhibit excellent insulation performance but they are limited to the temperature range to which their components – reflective foils and spacer materials – are compatible. For high temperature applications, the **i**nternal **m**ulti-screen **i**nsulation – IMI – has been developed that utilizes unique ceramic material technology to produce reflective screens with high temperature stability. For analytical insulation sizing a parametric material model is developed that includes the main contributors for heat flow which are radiation and conduction. The adaptation of model-parameters based on effective steady-state thermal conductivity measurements performed at NASA Langley Research Center (LaRC) allows for extrapolation to arbitrary stack configurations and temperature ranges beyond the ones that were covered in the conductivity measurements. Experimental validation of the parametric material model was performed during the thermal qualification test of the X-38 Chin-panel, where test results and predictions showed a good agreement.

INTRODUCTION

IMI type insulation is an effective lightweight insulation whose main functional principle is the reduction of radiation heat transport by the use of reflective oxide-ceramic fibrous substrate membranes, double-side coated with a very thin (a few nm) noble metal coating. These reflective screens are separated by low density fibrous felts made of alumina oxides (Al_2O_3). The high temperature stability of the noble metal coated ceramic screens and the high temperature compatibility of the spacer material allows IMI to be used in high temperature applications up to

---

Weiland, Stefan, MT-Aerospace, Franz-Josef-Strauß-Straße 5, 86153 Augsburg, Germany
Handrick, Karin, Dr., MT-Aerospace, Franz-Josef-Strauß-Straße 5, 86153 Augsburg, Germany
Daryabeigi, Kamran, NASA Langley Research Center, MS 190, Hampton, Virginia, 23681, USA

1700°C. IMI insulations have the inherent advantage of adaptability to specific needs. Depending on the desired insulation performance, the stack of screens and intermediate spacer felts can be configured with more or less screens separated either by thick or thin spacer mats. During the development process and in the frame of IMI material characterisation activities, the effective thermal conductivity of several IMI insulation packages has been measured in steady-state conditions at LaRC. These measurement results served as a basis for the development of a simplified parametric material model that allows a temperature and pressure dependent computation of the thermal conductivity including an extrapolation to high temperatures and arbitrary stack configurations.

IMI THERMAL CONDUCTIVITY TESTS AT LARC

At LaRC, steady state effective thermal conductivity tests have been performed by a testing technique based on the ASTM C-201 standard [1]. The thermal conductivity testing apparatus facilitates measurements at environmental pressures from 0.013 Pa to 1E5 Pa. The temperature at the hot sample side can be varied between room temperature up to 1000°C whereas the cold sample side is maintained close to room temperature. The test apparatus is described in [2]. Figure 1 shows a schematic of the test setup. The heater surface can be heated up to temperatures of about 1100°C by multiple rows of iron-chrome-aluminum heater wires. Since the heater plate does not provide a uniform temperature distribution, a septum plate made from INCONEL 625 is used to provide a uniformly heated boundary, which is placed directly on top of the test sample. Temperature information is retrieved from thermocouples installed on top of the septum plate in order to ensure an undisturbed contact between the septum plate and the test sample. At the "cold" side, a water-cooled aluminium plate equipped with multiple thin-film heat flux gages serves as the cold boundary. Thermocouples at the aluminium plate provide a temperature reading of the cold side.

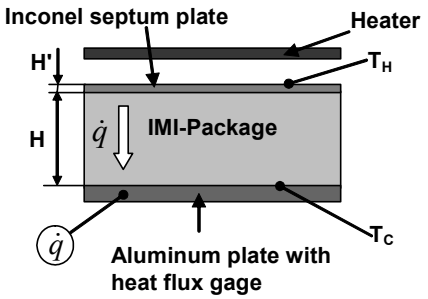

Figure 1: Schematic of the Thermal Conductivity Test Apparatus

Since the hot side temperature of the test samples is not measured directly but on the opposite side of the septum plate, the actual hot side temperature of the insulation specimens must be computed by taking into account the thickness and the known thermal conductivity of the INCONEL plate. The effective thermal conductivity of the sample is consequently computed by:

$$\lambda_{eff} = \frac{H}{\frac{T_H - T_C}{\dot{q}} - \frac{H'}{\lambda_{INCONEL}}} \quad (1)$$

where λ [W/(m.K)] denotes thermal conductivity, H [m] represents thickness, q [W/m^2] is heat flux, and T_H and T_C [K] represent the hot and cold boundary temperatures, respectively. The experimental investigation consisted of tests on several IMI samples with either gold or platinum coated screens. From the complete set of tested samples, a group of five had been selected for further investigation, which had in common the same type of spacer material, made from SAFFIL-fibers. The samples had dimensions of approximately 300 mm by 300 mm and a uniform height of approximately 20 mm. All IMI samples where bagged in a wrap of NEXTEL 440 cloth that had circular cut-outs at the "hot" and "cold" sides, with a diameter of 150 mm. Table I shows the main characteristics of the investigated IMI samples (called modules).

Effective thermal conductivity measurements have been conducted at nine different pressure steps from 0.1 Pa (0.001 torr) to 10^5 Pa (760 torr) and by varying the hot side boundary temperature in six steps from 100°C to 980°C by simultaneously maintaining the cold boundary temperature at room temperature. Thus, for each IMI module, a dataset of 9 x 6 = 54 data points has been delivered, containing the measured hot and cold side boundary temperatures as well as the computed mean temperature and the measured heat flux.

TABLE I: IMI SAMPLES TESTED AT LARC

Module No.	Screens		Spacers				Height [mm]
	Mat.	Number.	Mat.	ρ [kg/m^3]	Thickness [mm]	Number	
1	Au	5	Saffil	24	4	5	22
7	Pt	5	Saffil	24	4	5	23
9	Pt	10	Saffil	24	2	10	23
10	Pt	10	Saffil	48	2	10	24
12	Pt	5	Saffil	48	4	5	26

TEST DATA PROCESSING

As already stated, the experimental investigations resulted in a data package for each IMI module, incorporating the cold and the hot side boundary temperature, the computed mean temperature, as well as the measured heat flux and the corresponding effective thermal conductivity, which was computed using Eq. (1), or in a more general sense, without taking into account the special situation of the test set up with the INCONEL septum plate:

$$\lambda_{eff} = \dot{q}\frac{H}{T_H - T_C} \quad (2)$$

For developing a parametric material model, it is necessary to convert the effective thermal conductivities into local thermal conductivities $\lambda(T)$. This conversion has been performed by modelling the local thermal conductivity by a polynomial function, choosing the order of the polynomial equal to the number of experimentally determined data points reduced by one (n – 1):

$$\lambda(T) = \sum_{i=0}^{n-1} a_i T^i \qquad (3)$$

With the known set of data points for T_{H_i}, T_{C_i} and λ_{eff_i} (i = 1..n) the unknown coefficients of the polynomial for $\lambda(T)$ are determined by substituting the model function Eq. (3) into Eq. (4):

$$\lambda_{eff\_i} = \frac{1}{T_{H\_i} - T_{C\_i}} \int_{T_{C\_i}}^{T_{H\_i}} \lambda(T) dT \qquad (4)$$

Integrating the polynomial model function according to Eq. (4) and rearranging leads to a system of linear equations:

$$\left(A_{ij}\right) \begin{pmatrix} a_0 \\ \vdots \\ a_{n-1} \end{pmatrix} = \begin{pmatrix} \lambda_{eff\_1} \cdot \left(T_{H\_1} - T_{C\_1}\right) \\ \vdots \\ \lambda_{eff\_n} \cdot \left(T_{H\_n} - T_{C\_n}\right) \end{pmatrix} \qquad (5)$$

with the matrix elements:

$$A_{ij} = \frac{1}{j}\left(T_{H\_i}^{j} - T_{C\_i}^{j}\right) \qquad (6)$$

Solving the system of Eq. (5) for the unknown coefficients (a_0 to a_{n-1}) leads to the function $\lambda(T)$. It must be mentioned that this function is only valid in the temperature range that has been used for deriving $\lambda(T)$, therefore from T_{C_1} to T_{H_n}. Extrapolation to lower and higher temperatures is not possible. Also the resulting thermal conductivity function only applies to the particular stack configuration of the IMI module, where the data was derived from. The functional dependence of thermal conductivity on temperature worked out so far does not allow for an extrapolation to IMI modules having a different screen/spacer number or different spacer thickness and densities. Therefore, analysis work was performed to develop a simplified parametric material model that allows the computation of thermal conductivities for arbitrary IMI stack configurations.

DEVELOPMENT OF A SIMPLIFIED PARAMETRIC MATERIAL MODEL

Since the measurement of particular IMI insulation samples – characterized by a set of parameters - lacks the possibility to find thermal conductivity data for other insulation modules that have a different configuration, the need for a more general

mathematical material model emerges. Sizing and optimisation procedures for IMI type insulations require a mathematical relation between the IMI stack configuration and the corresponding thermal conductivity. The development of such a relation will be described in this section.

In general, the process of heat transfer in a medium where gas conduction, radiation heat transport and solid conduction appear simultaneously is quite complex and hard to describe by means of simplified mathematical equations. However, the main goal of the analysis task was to be able to obtain thermal conductivity values from an equation that would only need a few input variables for generating a thermal conductivity value.

Heat Transport by Gas Conduction in Porous Media

The thermal conductivity of a gas trapped in the interstitial space inside a porous media like a fibrous insulation felt is given by the temperature jump theory:

$$\lambda_{gas} = \frac{\lambda_{gas,0}}{1 + 2\frac{2-\alpha}{\alpha} \cdot \frac{2\kappa}{\kappa+1} \cdot \frac{1}{\mathrm{Pr}} \cdot \frac{\tilde{\lambda}}{L_c}} \qquad (7)$$

where α, κ, and Pr are the gas accommodation coefficient, the ratio of specific heats at constant volume and pressure, and Prandtl number, respectively. The variable $\lambda_{gas,0}$ stands for the thermal conductivity of the gas in free space, which may be a function of temperature. The mean free path, $\tilde{\lambda}$, of the gas is given by:

$$\tilde{\lambda} = \frac{k \cdot T}{\sqrt{2} \cdot \pi \cdot d_m^2 \cdot p} \qquad (8)$$

where k, d_m, and p are Boltzmann constant, gas collision diameter, and pressure, respectively. The characteristic length for the transport problem in a porous media is given by the following equation:

$$L_c = \frac{\pi}{4} \frac{D_f}{\rho / \rho_0} \qquad (9)$$

where D_f, ρ, and ρ_o are the fiber mean diameter, density of insulation spacer, and bulk density, respectively. Combining equations (7), (8) and (9), the thermal conductivity of the gas inside a fibrous insulation can be expressed by Eq. (10), where β is introduced for collecting terms from the above equations (7), (8) and (9):

$$\lambda_{gas} = \frac{\lambda_{gas,0}}{1 + \beta \cdot \rho \cdot \frac{T}{p}} \qquad (10)$$

The gas thermal conductivity in free space, $\lambda_{gas,0}$, is approximated by:

$$\lambda_{gas,0} = \frac{a \cdot T^b}{1 + \frac{c}{T}} \qquad (11)$$

where, according to theory, a = 0.0024 W/m/K$^{1.5}$, b = 0.5 and c = 123.6 K. However, this set of parameters has been found to be unsatisfactory showing a significant discrepancy between calculated and experimentally determined values. Therefore, the following parameters have been used: a = 8.97e-4 W/m/K$^{1.637}$, b = 0.637 and c = 84.12 K. These numbers give a good approximation to experimentally determined thermal conductivity of air between 300 and 1200 K. However, the use the second set of parameters in Eq. (11) results in underestimating thermal conductivity at temperatures above 1200 K.

Heat Transport by Radiation

In contrast to other conventional fibrous insulations the transport of heat through radiation is impaired by the use of reflective screens in combination with fibrous spacers. The radiation is therefore subject to multiple reflection and scattering. The mathematical formulation of the heat flow therefore takes into account this fact by combining terms due to re-reflection between a stack of mirrors and due to the extinction of radiation within the fibrous spacer felts. For a single cell made up from two screens and a spacer felt in between, the heat flow can be computed by [3,4]:

$$\dot{q} = \frac{\sigma \cdot n^2 \cdot \left(T_H^4 - T_C^4\right)}{\left(\frac{2}{\varepsilon} - 1\right) + \left(\frac{3}{4} \cdot e \cdot \rho \cdot d\right)} \qquad (12)$$

The index of refraction n in Eq. (12) has been assumed to be 1 which is close to actual values for SAFFIL. For a stack of multiple screens separated by spacers, the heat flow is reduced by the factor *1/(n+1).* The corresponding thermal conductivity of such a stack of reflective screens is:

$$\lambda_{rad} = \frac{4 \cdot \sigma \cdot T^3 \cdot d}{\left(\frac{2}{\varepsilon} - 1\right) + \left(\frac{3}{4} \cdot e \cdot \rho \cdot d\right)} \qquad (13)$$

The parameter d in this equation denotes the thickness of a single spacer, which comes from a simplification in the derivation of Eq. (13), since the total stack height divided by the term $n + 1$ simplifies to d. At this point it has to be mentioned that Eq. (13) is only valid for stacks having a constant spacer thickness, and optically thick spacers. The parameters ε and e, representing the foil emissivity and the spacer specific extinction [m²/kg], respectively, have been assumed to be linearly dependent on temperature, whereas the following functions are defined:

$$\varepsilon(T) = a_\varepsilon + b_\varepsilon \cdot T \text{ and } e(T) = a_e + b_e \cdot T \qquad (14)$$

Solid Conduction

Although material models exist that give a relation between the thermal conductivity of the fibrous material and the solid fraction and the parent material thermal conductivity, in developing a simplified material model, the thermal conductivity due to solid conduction has been assumed to be constant:

$$\lambda_{solid} = const. \quad (15)$$

PARAMETER FIT

For determining a set of parameters that describe the thermal conductivity of an arbitrary IMI insulation stack, a least squares method has been employed in order to find parameters that give the lowest possible differences between measured and calculated thermal conductivities, which are computed according to Eq. (16).

$$\lambda = \lambda_{solid} + K \cdot \lambda_{gas} + \lambda_{rad} \quad (16)$$

The parameter K has been introduced at this point to take into account possible coupling effects between radiation and conduction [4].

Table II provides the parameters found for the IMI-modules investigated. Concerning the set of parameters, those coefficients that determine the spacer specific extinction have been left out from the process of finding optimum values. Instead, the provided numbers for a_e and b_e represent data, which were taken from literature [3]. Consequently, the search for parameters was limited to the following parameters: β, a_ε, b_ε, λ_{solid} and K.

TABLE II: RESULTS FROM PARAMETER FIT

Param.	Mod.1	Mod. 7	Mod. 9	Mod. 10	Mod. 12
β [J/kg/K]	0.0079	0.0096	0.0121	0.0088	0.0065
a_ε [/]	0.0387	0.0991	0.1	0.0381	0.0534
b_ε [1/K]	7.84e-5	8.86e-5	1.3e-4	1.37e-4	1.09e-4
a_e [m²/kg]	36.25	36.25	36.25	36.25	36.25
b_e [m²/kg/K]	0.0125	0.0125	0.0125	0.0125	0.0125
λ_{solid} [W/m/K]	0.0031	0.0024	0.0018	0.0022	0.0019
K [/]	1.16	1.18	1.22	1.09	0.93

The graphs in Figure 2 compare the measured thermal conductivities that have been converted to local thermal conductivities of two IMI modules for different pressures to the predicted results using the parametric material model. As can be seen in Table II, the parameters found for the different IMI modules exhibit some scatter, even within those modules having the same spacer density but different spacer thickness. For sizing purposes a single set of parameters has been established by collecting the most unfavourable numbers found for each parameter. In addition, it has to be stated that the parameters obtained so far are valid for IMI insulation in

an un-aged state. During the development of the IMI type insulation it has been discovered that the optical properties of the reflective foils are susceptible to ageing effects that globally reduce the insulation efficiency of IMI when repeatedly used at high temperatures. This effect is considered in the material model, by an increased foil emissivity. Supported by calorimetric and IR-optical measurements [4], an aged foil emissivity for gold has been determined that can be approximated by $\varepsilon = 0.14 + 6 \cdot 10^{-5} K^{-1} \cdot T$. The corresponding aged emissivity for platinum is constant at ε = 0.45. These values have been obtained after an extended thermal ageing such that further thermal exposures did not lead to higher emissivity values. It can be considered as the worst conceivable material condition.

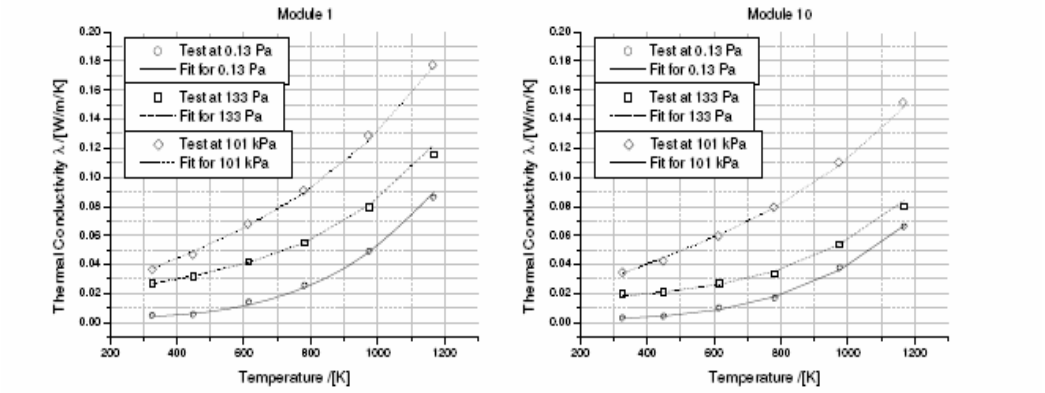

Figure 2. Local Thermal Conductivity of Modules 1 and 10 – Comparison between Model and Test Results

MATERIAL MODEL VALIDATION

The material model as described before has been validated in the frame of the qualification test activities of the X-38 Chin panel, which where conducted during year 2001. As part of a series of qualification tests, thermal tests were performed in order to verify the concept of the thermal protection system. As a part of the insulating system, an IMI-stack was used as the outermost – and consequently most loaded – layer. This IMI module consisted of 20 platinum foils separated equally by SAFFIL spacers, having a density of 48 kg/m³. For handling and integration purposes, the IMI stack was bagged in a NEXTEL 440 cloth, which had a fabric thickness of 0.765 mm. Underneath the IMI package, two additional layers of insulation were placed, a 10.6-mm-thick HTI (high temperature insulation) and a 20-mm IFI (internal flexible insulation) insulation package. These two types of insulation are based on Al_2O_3 fiber felts, supplied by ASTRIUM [6]. At the lowermost, an aluminium plate was situated as a pure heat sink. Figure 3 shows a schematic of the insulation configuration.

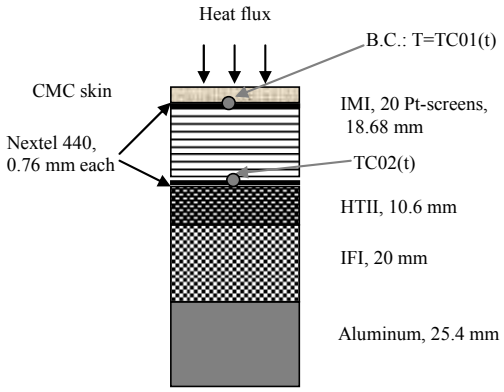

Figure 3: Schematic of the X-38 Chin Panel Insulation System

The test sample was equipped with numerous thermocouples for reading out temperature values at distinct locations. The first thermocouple of particular interest, denoted as TC01, was placed directly underneath the covering ceramic matrix composite – CMC - Chin panel. The temperature reading from this thermocouple was later used as boundary condition in the simulation of the tests, since it represented the temperature at the hot side of the IMI-insulation stack. The second thermocouple, denoted as TC02, was placed in between the IMI insulation and the underlying HTI-insulation. This temperature reading represents the cold side temperature of the IMI stack and was later used for correlation between the simulation and test results.

There were three main test runs carried out during the campaign, but for evaluation purposes only test run 1 and run 3 were used because during test run 2 some difficulties with the test equipment occurred (water leakage in the cooling system) with an unknown effect on the test results. The tests were carried out in principle by electrically heating the outer CMC skin of the test specimen according to a specified temperature profile and measuring the temperature response at different locations of particular interest. Simultaneously, the environmental pressure was varied. More detailed information concerning the test facility is available at [5].

Figure 4 presents at its left the measured temperature histories for TC01 and TC02 as well as the pressure evolution during the test run 1. In addition, the analytical simulation results for TC02 are plotted in the diagram that have been obtained by using the material model described above, valid for new IMI. It can be seen that the simulation of TC02 slightly overestimated the temperatures but a good correlation was achieved overall with a root mean square deviation of approximately 19 K. Test run 3 was carried out with a similar temperature profile for TC01, but with a considerably steeper pressure rise during the test. The right portion of Figure 4 shows the temperature and pressure histories. A direct comparison to test run 1 reveals a lower peak temperature for TC01 but a steeper temperature rise for TC02. The simulation of TC02 for test run 3 has been performed by using the IMI material model, taking into account the optical properties for aged foils, with $\varepsilon = 0.45$. The outcomes of this simulation are also plotted on the right side of Figure 4. It can be seen that there is a slight

underestimation for TC02, however the RMS- deviation between measurement and simulation of TC02 is approximately 13 K.

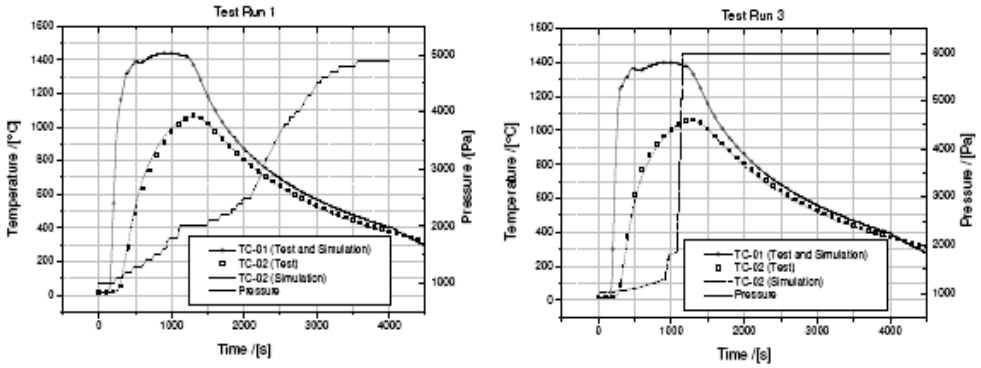

Figure 4: Comparison between Simulation and Test

CONCLUSION

A parametric material model was developed for modelling heat transfer through IMI insulations based on effective thermal conductivity measurements on five IMI modules. The parametric model material enabled extrapolation to arbitrary stack compositions and to higher temperatures. A series of transient thermal tests were used to validate the parametric material model. Regarding the transient test results, the simulations of temperatures at thermocouple location TC02 in test run 1 as well as in test run 3 show good agreement with the experimental values. Since the actual IMI-stack used in these tests consisted of 20 Pt screens and was exposed to temperatures up to 1400°C, a substantial extrapolation with respect to thermal conductivity was performed, since the material model had been "calibrated" with steady-state test results covering temperatures up to 980°C and IMI-modules with only 10 screens. Regarding the ageing effect of the IMI reflective screens, the use of optical properties of aged Pt-screens that were determined by calorimetric and IR-optical tests seems to be appropriate. However, uncertainty exists about the degree of aging. The applied emissivity for aged Pt-screens was according to emissivity measurements [4] after more than 7 to 10 temperature cycles, where in contrast the IMI stack in the Chin panel test has only experienced three cycles. Potentially, the presence of high humidity caused by the water leakage during test run 2 in combination with high temperatures may have led to an enforced surface deterioration.

REFERENCES

1. Standard Test Method for Thermal Conductivity of Refractories, *Annual Book of ASTM Standards,* Vol. 15.01, American Society for Testing and Materials, West Conshohocken, PA, pp. 54-59, 2000.
2. Daryabeigi, K., "Analysis and Testing of High Temperature Fibrous Insulation for Reusable Launch Vehicles," AIAA 99-1044, January 1999.
3. "Wärmetransport in Isolationssystemen extrem hoher spezifischer Extinktion," Physikalisches Institut Würzburg, Report E21-0288-2, 1988.
4. "Bayrisches Zentrum für angewandte Energieforschung e.V., Bericht über kaloriemetrische und IR-optische Messungen an Hermes Reflektorfolien für MAN Technologie AG," Report ZAE 2-1292-1, 1992.
5. Hilfer, G., "Thermomechanical Ground Testing for X-38 Flight Qualification," Second International Symposium on Atmospheric Reentry Vehicles and Systems, Arcachon, France, March 2001.
6. Antonenko, J., Müller M., "High Temperature Insulations on the X-38 Re-Entry Vehicle," 4th European Workshop: Hot Structures and Thermal Protection Systems for Space Vehicles, Palermo, Italy, November 2002.